

pubs.acs.org/macroletters Letter

Flow Optimization of Photoredox-Mediated Metal-Free Ring-Opening Metathesis Polymerization

Vincent P. Rigoglioso and Andrew J. Boydston*



Cite This: ACS Macro Lett. 2023, 12, 1479-1485



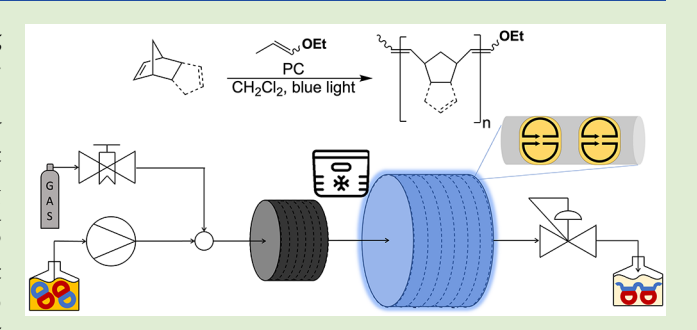
ACCESS I

III Metrics & More

Article Recommendations

SI Supporting Information

ABSTRACT: Photoredox-mediated metal-free ring-opening metathesis polymerization (MF-ROMP) is a convenient metal-free method to produce a variety of ROMP polymers. Transitioning MF-ROMP from a batch to a continuous flow process has yet to be demonstrated and could potentially benefit the production efficiency, safety, and modularity of reaction conditions. We designed and evaluated continuous flow and droplet flow setups and compared the results for MF-ROMP across a short series of common monomers. By using the droplet flow reactor setup, we achieved flow conversions comparable to that of batch and circumvented issues with diffusion-limited mixing and air exposure.



In general, products of ring-opening metathesis polymerization (ROMP) are used industrially in applications where their material strength and chemical compatibility are featured. Until recently, essentially all ROMP products were produced via metal-mediated mechanisms that employ any number of well-established metal—alkylidene initiators or transition metal salts (precatalysts). Although metal-mediated ROMP has been integrated into flow chemistry production methods (Figure 1a), the metal-free variant, which features several mechanistic distinctions from metal-mediated ROMP, has not yet been reported in flow (Figure 1c). 12,13

Flow chemistry is becoming increasingly more applicable for polymer production relative to batch reactor methods for its improved safety, ease of scale-up, and compatibility with automation. As breakthroughs in catalysis continue to enable more efficient chemical syntheses, so too have flow reactor designs advanced to augment and facilitate manufacturing processes. 14-21 Of course, certain classes of reactions present greater potential benefits from moving into a flow reactor process in comparison with batch production. For example, photochemical methods are best conducted with sufficient light penetration throughout the reactor volume, which is better accommodated by narrow diameter flow paths than by large volume batch reactors. 22-24 Additionally, reaction parameters, such as temperature, pressure, and thermal management, can be compartmentalized to small volumes at any given time within a flow reactor design, whereas the entirety of a batch reactor must be subjected to the requisite conditions.²⁵⁻³¹ We found light penetration, temperature control, and gas dissolution (e.g., conducting a reaction under nitrogen vs ambient air) to be particularly alluring features of flow chemistry when considering the potential

scale-up of photoredox-mediated metal-free ring-opening metathesis polymerization (MF-ROMP). At present, MF-ROMP is best conducted using photoredox catalysis, provides the highest yields for common monomers only when performed at low temperatures, and is particularly sensitive to the composition and concentration of gases in the reaction solvent.^{32–36}

As presented in Figure 1d, MF-ROMP proceeds through a radical cationic polymerization pathway that uses organic monomers, initiators, and photocatalysts. The polymerization proceeds under ambient conditions and performs worse under atmospheres of entirely nitrogen or oxygen, based upon total monomer conversion. 33 In this polymerization pathway, the 2,4,6-tris(4-methoxyphenyl)pyrylium tetrafluoroborate photocatalyst (2) serves as a photooxidant to generate the radical cationic enol ether (3) from the ethyl-1-propenyl ether initiator (1). This radical cationic intermediate engages and opens the strained bicyclic intermediate (4) to produce a ringopened olefin (5). This newly formed olefin maintains its radical cationic enol ether, which can go on to engage other monomer units to produce ROMP polymers. During this process, back-electron transfer from the reduced photocatalyst and degenerative electron transfer from neutral enol ethers are each envisioned, offering a photomediated, spatiotemporally

Received: September 12, 2023 Accepted: October 16, 2023



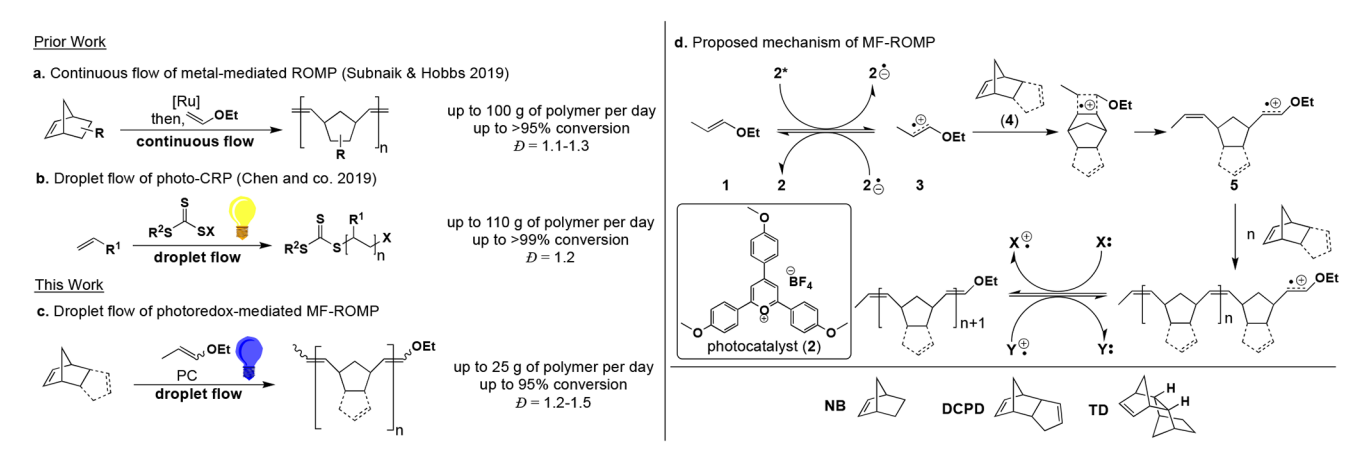


Figure 1. Supporting precedence for conducting MF-ROMP in a droplet flow setup. (a) The first literature example of metal-mediated ROMP in continuous flow. (b) The first literature example of a photocontrolled radical polymerization (CRP) in droplet flow. (c) This work. (d) Mechanism of MF-ROMP. X is the reduced pyryl radical or neutral enol ether; $Y^{\bullet+}$ is the excited photocatalyst or oxidized enol ether. Evaluated monomers pictured on the bottom.

controlled polymerization with living characteristics.¹³ Also noteworthy, only highly strained alkenes show conversion in MF-ROMP, leaving less-strained alkenes intact, enabling access to valuable ROMP polymers that are typically difficult to produce via metal-mediated pathways, such as linear poly-(dicyclopentadiene) (pDCPD).^{37–44} MF-ROMP has been demonstrated to produce high-conversion linear pDCPD, with the caveat of requiring low temperatures, which presents an opportunity for improvement with an appropriate flow process.

The scalability of linear pDCPD production and more generally of MF-ROMP, which is promoted by uniform irradiation and rapid cooling, would greatly benefit from the improved photophysics and heat transfer of flow chemistry relative to batch. 45-47 However, implementing MF-ROMP in flow has many of the obstacles associated with laboratory-scale flow reactors. Going from laboratory-scale batch photopolymerizations to laboratory-scale flow photopolymerizations is nontrivial, but there are well-defined parameters to consider when making the transition. 48-57 Mixing speed, irradiation setup, temperature control, reaction atmosphere, reactor size, and reaction time (among other things) must be considered in batch reactors. Similarly for flow reactors, the flow rate, irradiation setup, temperature control, reactor pressure, tubing diameter, and residence time must be considered. Being at subindustrial scales already creates further constraints and considerations for flow reactors. For transitioning MF-ROMP to a flow setup, we considered the benefits and limitations of both continuous and droplet flow reactor designs, which included the quality of mixing, control over reaction atmosphere, and throughput of the reactor.

Continuous flow reactor designs are commonly used at research scales, and reagent quantities necessitate slower flow rates. These subindustrial continuous flow reactors are typically limited to laminar flow, resulting in slow, diffusion-limited mixing within the reactor. This is detrimental to photopolymerizations because light exposure is uneven across the flow reactor, leading to increased molecular weight dispersities, reduced initiation efficiencies, and reduced monomer conversions (Figure 2). Though these issues can be mitigated by decreasing the flow loop diameter to improve diffusive mixing, doing so can drastically raise the pressure of the flow system and increase the likelihood of clogging,

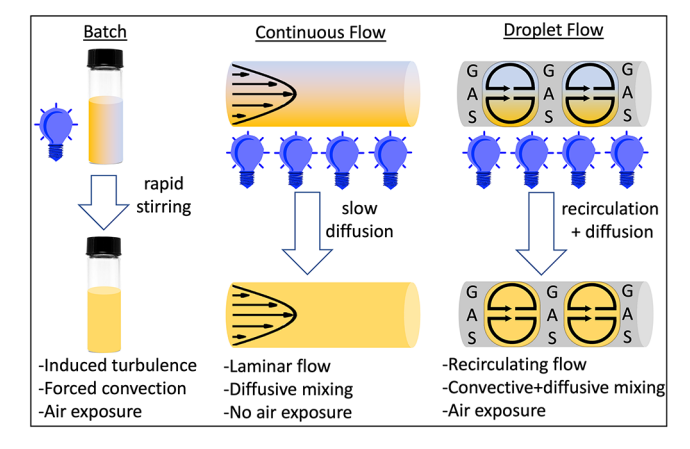


Figure 2. Comparison of batch, continuous flow (in the laminar flow regime), and droplet flow reactor setups upon exposure to irradiation. Flow velocity profiles shown in black for continuous and droplet flow.

especially in cases in which the solution viscosity increases as the polymerization progresses. There is also limited air exposure in continuous flow which, after observing nontrivial effects of reaction atmosphere on MF-ROMP, we thought could affect catalyst turnover.³³ Based on these observations, we hypothesized that a droplet flow reactor could be an ideal setup for MF-ROMP.

Droplet flow, sometimes referred to as Taylor flow, segmented flow, or isolated plug flow, refers to a flow reactor setup where two immiscible fluids (such as liquid/liquid or liquid/gas) are driven through the same flow loop. 66-69 The two fluids travel through the loop as separate, alternating plugs, causing each plug to circulate and mix within itself. In the case where one fluid is the reaction solution and the other fluid is a gas, the gas composition of the reaction solution can be maintained within the flow loop, thereby allowing one to probe the interaction of the atmosphere with a reaction. For polymerizations, droplet flow setups have been shown to yield experimental results (like molecular weight dispersity, monomer conversion, and initiation efficiency) better than that of continuous flow setups and comparable to that of small-scale batch setups owing to more similar mixing dynamics to that of batch. 66,67 Droplet flow setups have also shown great

compatibility with photocontrolled radical polymerizations (CRPs; Figure 1b). 70,71

The droplet flow setup is more complex than its continuous flow counterpart. Pressure regulators, flow controllers, and other safety measures are essential to creating a safe and controlled droplet flow setup. Another feature intrinsic to droplet flow is a reduced active reactor volume relative to continuous flow since part of the reactor volume is taken up by gas pockets. Though not explicitly studied here, others have shown that decreasing the gas to liquid ratio can maintain the mixing benefits of droplet flow while increasing the amount of active reactor volume.⁶⁹ When the optimal reactor setup is droplet flow, the decreased active volume is compensated by increased quality of mixing, translating to increased monomer conversion, increased initiator efficiency, and decreased dispersity relative to continuous flow. Based on our experience with MF-ROMP, droplet flow was viewed as a promising approach to outperform batch production methods. Herein, we report on laboratory-scale flow systems for MF-ROMP. We include comparisons of continuous versus droplet flow designs, optimization of flow conditions, and demonstration of successful (co)polymerizations using commercially relevant monomers.

For our studies, we evaluated norbornene (NB) and dicyclopentadiene (DCPD) as representative monomers for MF-ROMP before evaluating tetracyclododecene (TD) in our optimized flow setup. Importantly, NB performs well at room temperature and with high rates of monomer conversion relative to other MF-ROMP monomers. Therefore, NB is a good starting test-bed for comparing flow reactor designs. DCPD requires more stringent reaction conditions in batch production, such as low temperature, which makes it an attractive target for vetting modifications to flow systems. MF-ROMP of TD is unreported and demonstrates the applicability of our optimized flow setup to other monomer systems.

We assembled a modular flow reactor ensemble (Figure 3) and evaluated three flow reactor configurations for each

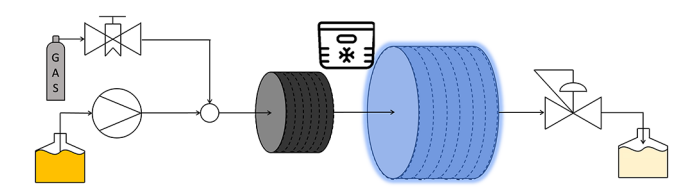


Figure 3. Flow reactor setup. The equipment shown on the scheme is reagent solution storage vessel, liquid pump, gas supply, needle valve, tee joint, temperature equilibration zone, active irradiation zone, chiller, back pressure regulator, and product solution storage vessel.

monomer system: (i) a continuous flow setup (CF) in which the reaction solution is pumped through the flow reactor; (ii) a droplet flow air setup (DF-Air) in which the reaction solution and dried air are pumped through the flow reactor; and (iii) a droplet flow nitrogen setup (DF-N₂) in which the reaction solution and dried nitrogen are pumped through the flow reactor. Within each flow setup, the gas flow rate, liquid flow rate, temperature, and system pressure could be directly controlled. When surveying different reagent concentrations, we found that higher concentrations of monomer led to large changes in viscosity during polymerization and that photocatalyst solubility was limited. Therefore, with our current designs, we chose to study more dilute concentrations. We

evaluated each monomer across the three different flow reactors to compare monomer conversion, product molecular weight, and polymer yield.

As we began our investigations of flow systems, we first focused on CF, as this design is comparatively simpler than DF. Although results with NB as the monomer were initially encouraging (reaching 80% conversion), attempts to reach serviceable yields when using DCPD as the monomer or comonomer (with NB) were met with limited success (Figure 4). We achieved only 37% conversion with DCPD alone (at $-20~^{\circ}\text{C}$) and 45% conversion with a 1:1 feed ratio of NB and DCPD (at $-20~^{\circ}\text{C}$). Much greater gains were found as we shifted focus to DF experiments, as described below.

The results from studying norbornene in DF, as summarized in Figures 4 and 5, and elaborated in Table S3.1, revealed that using a backpressure regulator (BPR) with the DF-Air setup resulted in low monomer conversions and significant photobleaching for the reaction mixture, which we ascribed to decomposition of the pyrylium salt photocatalyst. Specifically, NB conversion dropped from 67% to 60% to 51% as BPR pressure increased from 5 to 20 to 40 PSI (Figure 5). In the absence of a BPR, monomer conversions varied broadly across experiments, and the fickleness of the system precluded additional optimization. Lowering the temperature from room temperature to 0 °C at 40 PSI did not improve conversions when using the DF-Air setup (29% conversion, Table S3.1, entry 9).

We observed color loss to a lesser extent after changing the gas from air to nitrogen, signifying less photocatalyst decomposition. Accordingly, monomer conversion also increased, reaching above 80% for the 5, 20, and 40 PSI BPR experiments. Across the different setups that used a BPR and N₂, no significant trends in conversion were observed when varying the BPR pressure. As mentioned previously, oxygen has a nontrivial effect on MF-ROMP, and presumably using BPRs to pressurize the system in our studies causes an increased O2 concentration in the reaction solution, thereby causing an increased rate of photocatalyst decomposition. Decreasing solution temperature also increases dissolved O₂ concentration, and therefore, the observations regarding monomer conversion, pressure, and temperature support the hypothesis that increasing dissolved O2 concentration negatively affects the performance of these pressurized reactor setups. In general, when compared with continuous flow, droplet flow yielded better monomer conversions. The production of DF-N2, as compared to continuous flow, was lower, as is expected when using the same total flow rate but about a one-third the solution flow rate.

In the flow optimization of DCPD in Table S3.2, we noticed an influence of the total flow rate on conversion. Figure S3.2 shows that an appropriate balance needs to be found between the residence time and flow rate, which impacts mixing effects and reaction time. Batch control experiments corroborate the significant effects that mixing has on DCPD polymerization (Table S3.3). With DCPD, we found that higher flow rates, but shorter residence times were necessary for good conversions, observing 61% conversion for 0.56 mL/min total flow rate versus 34% and 50% conversion for 0.19 and 0.25 mL/min total flow rates, respectively (Table 1, entry 5; Table S3.2, entries 4 and 5). In flow experiments with DCPD performed in a cooled flow setup without a temperature equilibration zone, we observed low (<30%) monomer conversions (Table S3.2,

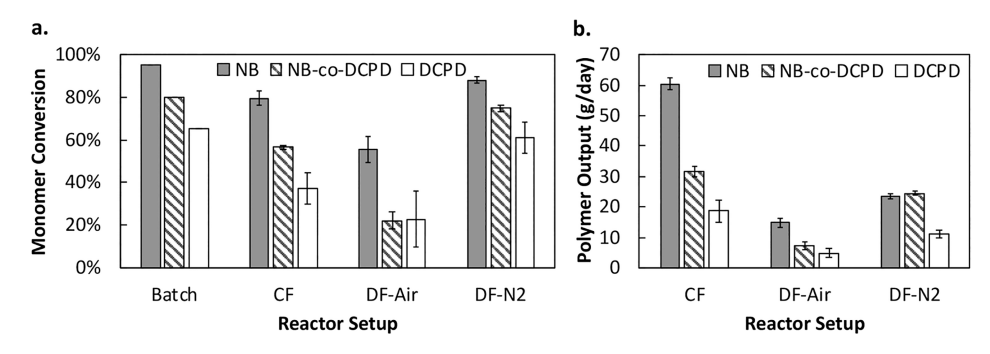


Figure 4. MF-ROMP reactor comparison: (a) Monomer conversion and (b) equivalent polymer output. Values are shown as average of 2 trials \pm standard deviation. For the NB experiments (solid, gray), NB:1:2 = 65:1:0.05; NB = 0.65 M; total flow rate for CF and DF = 0.9 mL/min; liquid flow rate for DF = 0.3 mL/min. For the DCPD experiments (solid, white), DCPD:1:2 = 25:1:0.07; DCPD = 0.45 M; total flow rate for CF and DF = 0.6 mL/min; liquid flow rate for DF = 0.2 mL/min. For the NB-co-DCPD experiments (striped, gray), NB:DCPD:1:2 = 25:25:1:0.07; [NB] = 0.3 M; total flow rate for CF and DF = 0.6 mL/min; liquid flow rate for DF = 0.2 mL/min.

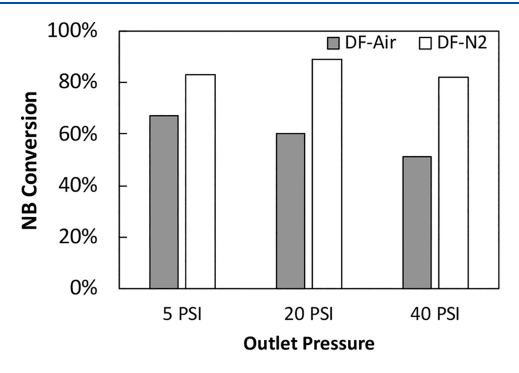


Figure 5. Droplet flow optimization: Gas, pressure, and temperature trends. NB:1:2 = 65:1:0.05; [NB] = 0.65 M; total flow rate = 0.9 mL/min; liquid flow rate = 0.3 mL/min.

entry 2), which we attribute to premature initiation of the polymerization before sufficient cooling.

After achieving successful polymerizations of both NB and DCPD, we extended our results to longer experiments, larger molecular weights, higher conversions, and different (co)-polymerizations. By extending the flow parameters of the DCPD homopolymerization to the copolymerization of NB and DCPD, we achieved 68% conversion of DCPD, 83% conversion of NB, and 75% total monomer conversion at -20 °C (Table 1, entry 7; Table S3.4, entry 4). We were also able to maintain the DF-N₂ setup for 5 h and achieved similar

conversions to the 1 h experiments (82% for NB, 55% for DCPD, and 74% for NB-co-DCPD Table 1, entries 2, 6, and 8). With these 5 h experiments, a slight drift in conversion was observed presumably due to increased moisture exposure of the storage vessel, which filled with air as the reaction solution pumped through the reactor (see Figure S3.6). We then extended our optimized DF-N2 conditions to increased loadings of NB, to increased conversions of NB and to TD. For NB, we achieved 74% monomer conversion and reached a number-average molecular weight of 19.3 kDa (notably above NB's entanglement molecular weight) at a polymer dispersity of 1.3 (Table 1, entry 3). We also lowered loadings of NB while increasing the residence time to achieve 95% monomer conversion via DF-N₂ (Table 1, entry 4). For TD after adjusting solvent and reagent concentrations to accommodate the pTD's solubility behavior, we achieved a similarly successful flow polymerization, reaching 74% monomer conversion at a projected output of 10 g/day of pTD (Table 1, entry 9).

After finding suitable setups for the NB, DCPD, and NB-co-DCPD polymerizations with respect to flow rate, residence time, and temperature, we were able to compare the observed flow performance trends, as summarized in Figure 4 and Table 1. In all cases, we saw that the DF-N₂ setup performed the best in terms of monomer conversion, reaching up to 95% for NB, 61% for DCPD, and 75% for NB-co-DCPD. Regarding polymer output, the continuous flow setup tended to do well

Table 1. Summarized Results of MF-ROMP via DF-N2

entry ^a	NB:DCPD:TD:1:2	residence time (min)	$conv^b$ (%)	$M_{\rm n}^{\ c} \ ({\rm kDa})$	Ð	$output^d$ (g/day)
1	65:0:0:1:0.05	28	88 ± 1	8.1 ± 0.6	$1.3 \pm 0.0(4)$	24 ± 1
2 ^e	65:0:0:1:0.05	30	82	7.7	1.3	22
3	200:0:0:1:0.05	30	74	19.3	1.3	20
4	25:0:0:1:0.05	45	95	3.3	1.3	17
5 ^f	0:25:0:1:0.07	45	61 ± 7	3.9 ± 0.7	1.3 ± 0.1	11 ± 1
$6^{e,f}$	0:25:0:1:0.07	45	55	3.4	1.4	10
7 ^f	25:25:0:1:0.07	45	75 ± 2	8.4 ± 1.0	1.4 ± 0.1	25 ± 1
$8^{e,f}$	25:25:0:1:0.07	45	74	8.4	1.4	17
9 ^g	0:0:25:1:0.07	50	74	5.8	1.5	10

[&]quot;Run at room temperature during a 1-h experiment at a liquid flow of 0.2-0.3 mL/min in a 25 mL active flow loop, unless otherwise noted. Values shown as an average of two trials \pm standard deviation when applicable. "Monomer conversion determined from ¹H NMR spectroscopy. "Number-average molecular weights (M_n) determined by GPC equipped with multiangle light-scattering detector and a measured dn/dc, as described in the Supporting Information. "S-h experiment. "Fun at -20 °C. "Run in ortho-dichlorobenzene."

because of its larger liquid flow rate, but the DF- N_2 setup was competitive in terms of output for DCPD-containing polymers, reaching up to 24 g/day for pNB, 11 g/day for pDCPD, and 25 g/day for pNB-co-DCPD. We confirmed that these flow experiments could be conducted for 5 h while maintaining similarly successful monomer conversions and polymer outputs. We also demonstrated that the DF- N_2 setup is compatible above the entanglement number-average molecular weight of NB, reaching 74% monomer conversion and achieving a number-average molecular weight of 19.3 kDa and a molecular weight dispersity of 1.3. Lastly, we then extended our optimized DF- N_2 conditions to TD where we achieved successful flow polymerization, reaching 74% monomer conversion at a projected output of 10 g/day of pTD.

We compared different flow setups for MF-ROMP using NB, DCPD, and TD monomer conversion as well as projected output as measurements of success. Through this process, we found that droplet flow configurations for MF-ROMP can translate results from small-scale batch experiments to flow processes. For polymerization of each monomer, droplet flow achieved higher conversion than continuous flow, which is attributed to a better quality of mixing in the former. On the other hand, within the constraints of the current scale, continuous flow gave greater quantities of projected daily polymer output due to the higher liquid flow rate in comparison with droplet flow. We found that lowering the reactive volume temperature was easily accommodated in flow, which offered benefits for MF-ROMP of DCPD. Similarly, solvent changes to enable MF-ROMP of TD were found to be straightforward. Moving forward, the reactor designs described herein can enable further scale-up of MF-ROMP while offering the operational and safety benefits of flow techniques for synthesis.

ASSOCIATED CONTENT

Supporting Information

The Supporting Information is available free of charge at https://pubs.acs.org/doi/10.1021/acsmacrolett.3c00545.

Materials, experimental procedures, spectral data, and additional figures (PDF)

AUTHOR INFORMATION

Corresponding Author

Andrew J. Boydston — Department of Chemistry, University of Wisconsin—Madison, Madison, Wisconsin 53706, United States; Department of Chemical and Biological Engineering, Department of Materials Science and Engineering, University of Wisconsin—Madison, Madison, Wisconsin 53706, United States; orcid.org/0000-0001-7192-4903;

Email: aboydston@wisc.edu

Author

Vincent P. Rigoglioso – Department of Chemistry, University of Wisconsin–Madison, Madison, Wisconsin 53706, United States

Complete contact information is available at: https://pubs.acs.org/10.1021/acsmacrolett.3c00545

Author Contributions

The manuscript was written through contributions of all authors. All authors have given approval to the final version of

the manuscript. CRediT: **Vincent Rigoglioso** conceptualization, data curation, formal analysis, investigation, methodology, validation, writing-original draft, writing-review & editing.

Notes

The authors declare the following competing financial interest(s): A.J.B. has an ownership interest in BCI, Inc., which has licensed the technology reported in this publication.

ACKNOWLEDGMENTS

We thank Promerus LLC for their generous gift of tetracyclododecene. We gratefully acknowledge financial support from the Army Research Office (W911NF-22-C0032), the National Science Foundation (CHE-2002886), and BCI, Inc. A.J.B. acknowledges partial financial support from the Yamamoto Family, the Office of the Vice Chancellor for Research and Graduate Education at the University of Wisconsin—Madison with funding from the Wisconsin Alumni Research Foundation. We are grateful to Frank Leibfarth (University of North Carolina at Chapel Hill) for helpful discussions. The following instrumentation in the Paul Bender Chemical Instrumentation Center was supported by Bruker AVANCE 400 NMR spectrometer by NSF CHE-1048642; Bruker AVANCE 500 NMR spectrometer by a generous gift from Paul J. and Margaret M. Bender.

REFERENCES

- (1) Mol, J. C. Industrial applications of olefin metathesis. *J. Mol. Catal. A: Chem.* **2004**, 213, 39–45.
- (2) Schrock, R. R. Synthesis of stereoregular polymers through ringopening metathesis polymerization. *Acc. Chem. Res.* **2014**, 47, 2457— 2466.
- (3) Sutthasupa, S.; Shiotsuki, M.; Sanda, F. Recent advances in ring-opening metathesis polymerization, and application to synthesis of functional materials. *Polym. J.* **2010**, *42*, 905–915.
- (4) Bielawski, C. W.; Grubbs, R. H. Living ring-opening metathesis polymerization. *Prog. Polym. Sci.* **2007**, 32, 1–29.
- (5) Rosebrugh, L. E.; Marx, V. M.; Keitz, B. K.; Grubbs, R. H. Synthesis of highly cis, syndiotactic polymers via ring-opening metathesis polymerization using ruthenium metathesis catalysts. *J. Am. Chem. Soc.* **2013**, *135*, 10032–10035.
- (6) Jeong, H.; Kozera, D. J.; Schrock, R. R.; Smith, S. J.; Zhang, J.; Ren, N.; Hillmyer, M. A. Z-Selective Ring-Opening Metathesis Polymerization of 3-Substituted Cyclooctenes by Monoaryloxide Pyrrolide Imido Alkylidene (MAP) Catalysts of Molybdenum and Tungsten. *Organometallics* 2013, 32, 4843–4850.
- (7) Forrest, W. P.; Axtell, J. C.; Schrock, R. R. Tungsten oxo alkylidene complexes as initiators for the stereoregular polymerization of 2, 3-dicarbomethoxynorbornadiene. *Organometallics* **2014**, *33*, 2313–2325.
- (8) Chauvin, Y. Olefin metathesis: The early days (Nobel lecture). *Angew. Chem., Int. Ed.* **2006**, 45, 3740–3747.
- (9) Schrock, R. R. Multiple metal-carbon bonds for catalytic metathesis reactions (Nobel lecture). *Angew. Chem., Int. Ed.* **2006**, 45, 3748-3759.
- (10) Grubbs, R. H. Olefin-metathesis catalysts for the preparation of molecules and materials (Nobel lecture). *Angew. Chem., Int. Ed.* **2006**, 45, 3760–3765.
- (11) Autenrieth, B.; Schrock, R. R. Stereospecific Ring-Opening Metathesis Polymerization (ROMP) of Norbornene and Tetracyclododecene by Mo and W Initiators. *Macromolecules* **2015**, *48*, 2493–2503
- (12) Subnaik, S. I.; Hobbs, C. E. Flow-facilitated ring opening metathesis polymerization (ROMP) and post-polymerization modification reactions. *Polym. Chem.* **2019**, *10*, 4524–4528.

- (13) Ogawa, K. A.; Goetz, A. E.; Boydston, A. J. Metal-Free Ring-Opening Metathesis Polymerization. *J. Am. Chem. Soc.* **2015**, *137*, 1400–1403.
- (14) Tonhauser, C.; Natalello, A.; Löwe, H.; Frey, H. Microflow Technology in Polymer Synthesis. *Macromolecules* **2012**, *45*, 9551–9570.
- (15) Parida, D.; Serra, C. A.; Gomez, R. I.; Garg, D. K.; Hoarau, Y.; Bouquey, M.; Muller, R. Atom Transfer Radical Polymerization in Continuous Microflow: Effect of Process Parameters. *J. Flow Chem.* **2014**, *4*, 92–96.
- (16) Den Haese, M.; Gemoets, H. P. L.; Van Aken, K.; Pitet, L. M. Fully biobased triblock copolymers generated using an unconventional oscillatory plug flow reactor. *Polym. Chem.* **2022**, *13*, 4406–4415.
- (17) Fortelný, I.; Juza, J. Description of the Droplet Size Evolution in Flowing Immiscible Polymer Blends. *Polymers* **2019**, *11*, 761.
- (18) Reis, M. H.; Leibfarth, F. A.; Pitet, L. M. Polymerizations in Continuous Flow: Recent Advances in the Synthesis of Diverse Polymeric Materials. *ACS Macro Lett.* **2020**, *9*, 123–133.
- (19) Plutschack, M. B.; Pieber, B.; Gilmore, K.; Seeberger, P. H. The Hitchhiker's Guide to Flow Chemistry. *Chem. Rev.* **2017**, *117*, 11796–11893.
- (20) Junkers, T. Precise Macromolecular Engineering via Continuous-Flow Synthesis Techniques. *J. Flow Chem.* **2017**, 7, 106–110.
- (21) Hu, X.; Zhu, N.; Fang, Z.; Guo, K. Continuous Flow Ring-Opening Polymerizations. *React. Chem. Eng.* **2017**, *2*, 20–26.
- (22) Elliott, L. D.; Berry, M.; Harji, B.; Klauber, D.; Leonard, J.; Booker-Milburn, K. I. A Small-Footprint, High-Capacity Flow Reactor for UV Photochemical Synthesis on the Kilogram Scale. *Org. Process Res. Dev.* **2016**, *20*, 1806–1811.
- (23) Herrero-Gomez, E.; van der Loo, C. H. M.; Huck, L.; Rioz-Martinez, A.; Keene, N. F.; Li, B.; Pouwer, K.; Allais, C. Photo-oxidation of Cyclopentadiene Using Continuous Processing: Application to the Photo-oxidation of Cyclopentadiene Using Continuous Processing: Application to the Synthesis of (1R,4S)-4-Hydroxycyclopent-2-en-1-yl Acetate. *Org. Process Res. Dev.* **2020**, 24, 2304–2310.
- (24) Aroh, K. C.; Jensen, K. F. Efficient kinetic experiments in continuous flow microreactors. *React. Chem. Eng.* **2018**, *3*, 94–101.
- (25) Gonzalez-Esguevillas, M.; Fernandez, D. F.; Rincon, J. A.; Barberis, M.; de Frutos, O.; Mateos, C.; Garcia-Cerrada, S.; Agejas, J.; MacMillan, D. W. C. Rapid Optimization of Photoredox Reactions for Continuous-Flow Systems Using Microscale Batch Technology. ACS Cent. Sci. 2021, 7, 1126–1134.
- (26) Rehm, T. H. Reactor Technology Concepts for Flow Photochemistry. *ChemPhotoChem.* **2020**, *4*, 235–254.
- (27) Sun, A. C.; Steyer, D. J.; Allen, R. A.; Payne, E. M.; Kennedy, R. T.; Stephenson, C. R. J. A droplet microfluidic platform for high-throughput photochemical reaction discovery. *Nat. Commun.* **2020**, *11*, 6202.
- (28) Harper, K. C.; Moschetta, E. G.; Bordawekar, S. V.; Wittenberger, S. J. A Laser Driven Flow Chemistry Platform for Scaling Photochemical Reactions with Visible Light. *ACS Cent. Sci.* **2019**, *5*, 109–115.
- (29) Andrews, S. R.; Becker, J. J.; Gagné, M. R. A Photoflow Reactor for the Continuous Photoredox-Mediated Synthesis of C-Glycoamino Acids and C-Glycolipids. *Angew. Chem, Int Ed.* **2012**, *51* (17), 4140–4143.
- (30) Su, Y.; Straathof, N. J. W.; Hessel, V.; Noël, T. Photochemical Transformations Accelerated in Continuous-Flow Reactors: Basic Concepts and Applications. *Chem.—Eur. J.* **2014**, *20*, 10562–10589.
- (31) Straathof, N. J W; Su, Y.; Hessel, V.; Noel, T. Accelerated gasliquid visible light photoredox catalysis with continuous-flow photochemical microreactors. *Nat. Protoc.* **2016**, *11*, 10–21.
- (32) Yang, X.; Murphy, L. M.; Haque, F. M.; Grayson, S. M.; Boydston, A. J. A highly efficient metal-free protocol for the synthesis of linear polydicyclopentadiene. *Polym. Chem.* **2021**, *12*, 2860–2867.
- (33) Goetz, A. E.; Pascual, L. M. M.; Dunford, D. G.; Ogawa, K. A.; Knorr, D. B.; Boydston, A. J. Expanded Functionality of Polymers

- Prepared using Metal-Free Ring-Opening Metathesis Polymerization. *ACS Macro Lett.* **2016**, *5*, 579–582.
- (34) Goetz, A. E.; Boydston, A. J. Metal-Free Preparation of Linear and Cross-Linked Polydicyclopentadiene. *J. Am. Chem. Soc.* **2015**, 137, 7572–7575.
- (35) Kensy, V. K.; Tritt, R. L.; Haque, F. M.; Murphy, L. M.; Knorr, D. B.; Grayson, S. M.; Boydston, A. J. Molecular Weight Control via Cross Metathesis in Photo-Redox Mediated Ring-Opening Metathesis Polymerization. *Angew. Chem., Int. Ed.* **2020**, *59*, 9074–9079.
- (36) Lu, P.; Kensy, V. K.; Tritt, R. L.; Seidenkranz, D. T.; Boydston, A. J. Metal-Free Ring-Opening Metathesis Polymerization: From Concept to Creation. *Acc. Chem. Res.* **2020**, *53*, 2325–2335.
- (37) Abadie, M. J.; Dimonie, M.; Couve, C.; Dragutan, V. New catalysts for linear polydicyclopentadiene synthesis. *Eur. Polym. J.* **2000**, *36*, 1213–1219.
- (38) Autenrieth, B.; Jeong, H.; Forrest, W. P.; Axtell, J. C.; Ota, A.; Lehr, T.; Buchmeiser, M. R.; Schrock, R. R. Z-Selective and Syndioselective Ring-Opening Metathesis Polymerization (ROMP) Initiated by Monoaryloxidepyrrolide (MAP) Catalysts. *Macromolecules* 2015, 48, 2480–2492.
- (39) Hayano, S.; Kurakata, H.; Tsunogae, Y.; Nakayama, Y.; Sato, Y.; Yasuda, H. Stereospecific Ring-Opening Metathesis Polymerization of Cycloolefins Using Novel Molybdenum and Tungsten Complexes Having Biphenolate Ligands. Development of Crystalline Hydrogenated Poly(endo-dicyclopentadiene) and Poly(norbornene). *Macromolecules* **2003**, *36*, 7422–7431.
- (40) Hayano, S.; Takeyama, Y.; Tsunogae, Y.; Igarashi, I. Hydrogenated Ring-Opened Poly(endo-dicyclopentadiene)s Made via Stereoselective ROMP Catalyzed by Tungsten Complexes: Crystalline Tactic Polymers and Amorphous Atactic Polymer. *Macromolecules* **2006**, *39*, 4663–4670.
- (41) Dono, K.; Huang, J.; Ma, H.; Qian, Y. Ring opening metathesis polymerization of dicyclopentadiene catalyzed by titanium tetrachloride adduct complexes with nitrogen-containing ligands. *J. Appl. Polym. Sci.* **2000**, *77*, 3247–3251.
- (42) Steese, N. D.; Barvaliya, D.; Poole, X. D.; McLemore, D. E.; DiCesare, J. C.; Schanz, J. J. Synthesis and thermal properties of linear polydicyclopentadiene via ring-opening metathesis polymerization with a third generation grubbs-type ruthenium-alkylidene complex. *J. Polym. Sci., Part A: Polym. Chem.* **2018**, *56*, 359–364.
- (43) Dumrath, C.; Dumrath, A.; Neumann, H.; Beller, M.; Kadyrov, R. Practical Ruthenium Catalysts for the Synthesis of Cyclic Olefin Oligomers, Polymers, and their Hydrogenated Derivatives. *Chem-CatChem.* **2014**, *6*, 3101–3104.
- (44) Yao, Z.; Wang, Z.; Yu, Y.; Zeng, C.; Cao, K. Facile synthesis and properties of the chemo-reversible and highly tunable metallogels based on polydicyclopentadiene. *Polymer* **2017**, *119*, 98–106.
- (45) Straathof, N. J. W.; Noël, T. Accelerating Visible-Light Photoredox Catalysis in Continuous-Flow Reactors. In *Visible Light Photocatalysis in Organic Chemistry*; Stephenson, C. R. J., Yoon, T. P., MacMillan, D. W. C., Eds.; Wiley-VCH: Weinheim, Germany, 2018; Chapter 13, pp 389–410.
- (46) Knowles, J. P.; Elliott, L. D.; Booker-Milburn, K. I. Flow photochemistry: Old light through new windows. *Beilstein J. Org. Chem.* **2012**, *8*, 2025–2052.
- (47) Aillet, T.; Loubiere, K.; Dechy-Cabaret, O.; Prat, L. Photochemical synthesis of a "cage" compound in a microreactor: Rigorous comparison with a batch photoreactor. *Chem. Eng. Process.* **2013**, *64*, 38–47.
- (48) Hook, B. D. A.; Dohle, W.; Hirst, P. R.; Pickworth, M.; Berry, M. B.; Booker-Milburn, K. I. A Practical Flow Reactor for Continuous Organic Photochemistry. *J. Org. Chem.* **2005**, *70*, 7558–7564.
- (49) Ramsey, B. L.; Pearson, R. M.; Beck, L. R.; Miyake, G. M. Photoinduced Organocatalyzed Atom Transfer Radical Polymerization Using Continuous Flow. *Macromolecules* **2017**, *50*, 2668–2674.
- (50) Buss, B. L.; Miyake, G. M. Photoinduced Controlled Radical Polymerizations Performed in Flow: Methods, Products, and Opportunities. *Chem. Mater.* **2018**, *30*, 3931–3942.

- (51) Rubens, M.; Latsrisaeng, P.; Junkers, T. Visible light-induced inferter polymerization of methacrylates enhanced by continuous flow. *Polym. Chem.* **2017**, *8*, 6496–6505.
- (52) Lauterbach, F.; Rubens, M.; Abetz, V.; Junkers, T. Ultrafast PhotoRAFT Block Copolymerization of Isoprene and Styrene Facilitated through Continuous-Flow Operation. *Angew. Chem., Int. Ed.* **2018**, *57*, 14260–14264.
- (53) Corrigan, N.; Almasri, A.; Taillades, W.; Xu, J.; Boyer, C. Controlling Molecular Weight Distributions through Photoinduced Flow Polymerization. *Macromolecules* **2017**, *50*, 8438–8448.
- (54) Chen, K.; Zhou, Y.; Han, S.; Liu, Y.; Chen, M. Main-Chain Fluoropolymers with Alternating Sequence Control via Light-Driven Reversible-Deactivation Copolymerization in Batch and Flow. *Angew. Chem., Int. Ed.* **2022**, *61*, No. e202116135.
- (55) Davidson, C. L. G.; Lott, M. E.; Trachsel, L.; Wong, A. J.; Olson, R. A.; Pedro, D. I.; Sawyer, W. G.; Sumerlin, B. S. Inverse Miniemulsion Enables the Continuous-Flow Synthesis of Controlled Ultra-High Molecular Weight Polymers. *ACS Macro Lett.* **2023**, *12*, 1224–1230.
- (56) Song, H.; Chen, D. L.; Ismagilov, R. F. Reactions in Droplets in Microfluidic Channels. *Angew. Chem., Int. Ed.* **2006**, 45, 7336–7356.
- (57) Casadevall i Solvas, X.; deMello, A. Droplet microfluidics: recent developments and future applications. *Chem. Commun.* **2011**, 47, 1936–1942.
- (58) Lima, M. J.; Silva, A. M. T.; Silva, C. G.; Faria, J. L.; Lopes, J. C. B.; Dias, M. M. An innovative static mixer photoreactor: Proof of concept. *Chem. Eng. J.* **2016**, 287, 419–424.
- (59) Gobert, S. R. L.; Kuhn, S.; Braeken, L.; Thomassen, L. C. J. Characterization of Milli- and Microflow Reactors: Mixing Efficiency and Residence Time Distribution. *Org. Process Res. Dev.* **2017**, 21, 531–542.
- (60) Danckwerts, P. V. Continuous flow systems: Distribution of residence times. *Chem. Eng. Sci.* **1953**, *2*, 1–13.
- (61) Angeli, P.; Gavriilidis, A. Hydrodynamics of Taylor flow in small channels: a review. *Proceedings of the Institution of Mechanical Engineers, Part C: Journal of Mechanical Engineering Science* **2008**, 222, 737–751.
- (62) Villermaux, E. Mixing Versus Stirring. Annu. Rev. Fluid Mech. 2019, 51, 245–273.
- (63) Rhee, M.; Burns, M. A. Membranous Bypass Valves for Discrete Drop Mixing and Routing in Microchannels. *Sensors & Transducers Journal* **2008**, 24, 590–601.
- (64) Chen, C.; Zhao, Y.; Wang, J.; Zhu, P.; Tian, Y.; Xu, M.; Wang, L.; Huang, X. Passive Mixing inside Microdroplets. *Micromachines* **2018**, *9*, 160.
- (65) Loizou, K.; Wong, V. L.; Hewakandamby, B. Examining the Effect of Flow Rate Ratio on Droplet Generation and Regime Transition in a Microfluidic T-Junction at Constant Capillary Numbers. *Inventions* **2018**, *3*, 54.
- (66) Reis, M. H.; Varner, T. P.; Leibfarth, F. A. The Influence of Residence Time Distribution on Continuous-Flow Polymerization. *Macromolecules* **2019**, *52*, 3551–3557.
- (67) Lu, S.; Wang, K. Kinetic study of TBD catalyzed δ -valerolactone polymerization using a gas-driven droplet flow reactor. *React. Chem. Eng.* **2019**, *4*, 1189–1194.
- (68) Schrimpf, M.; Esteban, J.; Warmeling, H.; Färber, T.; Behr, A.; Vorholt, A. J. Taylor-Couette reactor: Principles, design, and applications. *AIChE J.* **2021**, *67*, No. e17228.
- (69) Russum, J. P.; Jones, C. W.; Schork, F. J. Impact of Flow Regime on Polydispersity in Tubular RAFT Miniemulsion Polymerization. *AIChE J.* **2006**, *52*, 1566–1576.
- (70) Zhou, Y.; Gu, Y.; Jiang, K.; Chen, M. Droplet-Flow Photopolymerization Aided by Computer: Overcoming the Challenges of Viscosity and Facilitating the Generation of Copolymer Libraries. *Macromolecules* **2019**, *52*, 5611–5617.
- (71) Zhou, Y.; Fu, Y.; Chen, M. Facile Control of Molecular Weight Distribution via Droplet-Flow Light-Driven Reversible-Deactivation Radical Polymerization. *Chin. J. Chem.* **2022**, *40*, 2305–2312.